

UNCOVERING BENZOQUINONE DERIVATIVES FOR REDOX FLOW BATTERIES: DFT INSIGHTS ON REDUCTION POTENTIALS AND SOLVENT EFFECTS

Getachew Abera Negesse¹, Mesfin Diro Chaka², Desalegn Nigatu Gemechu¹, Gamachis Sakata Gurmesa³, Mekonnen Ababayehu Desta^{1*}, Ahmed Mustefa Mohammed¹ and Yedilfana Setarge Mekonnen^{4*}

¹Department of Chemistry, College of Natural and Computational Sciences, Addis Ababa University, P. O. Box 1176, Addis Ababa, Ethiopia

²Computational Science Program, College of Natural and Computational Sciences, Addis Ababa University, P. O. Box 1176, Addis Ababa, Ethiopia

³Department of Physics, College of Natural and Computational Science, Mattu University, P. O. Box 318, Mattu, Ethiopia

⁴Center for Environmental Science, College of Natural and Computational Sciences, Addis Ababa University, P. O. Box 1176, Addis Ababa, Ethiopia

(Received June 22, 2024; Revised October 27, 2024; Accepted November 6, 2024)

Abstract. Quinones possess high redox potential, making them suitable for organic redox-flow batteries. Their oxidation and discharge during charging involve two reversible electron transfer reactions. This study utilized density functional theory (DFT) with the B3LYP functional and 6-31G(d) basis set to calculate the first and second reduction potentials of benzoquinones (BQ). Various BQ derivatives were created by adding electron-donating substituents (-NHCH₃, -NH₂, -OCH₃, -NHCOCH₃, -OCOCH₃). The universal solvation model (SMD) assessed solvent effects, while lithium salts, solvation-free energy, and HOMO-LUMO energies influenced reduction potentials. The -OCOCH₃-substituted BQ showed the highest first and second redox potentials at 2.81 V and 2.27 V, respectively. Adding boron trifluoride (BF₃) salt increased these potentials to 3.99 V and 3.84 V. The electrochemical behavior of BQ and its derivatives was examined in three solvents: carbon tetrachloride (CCl₄), acetonitrile (ACN), and water (H₂O). The average reduction potentials in these solvents followed the trend CCl₄ < ACN < H₂O, with water being the most effective due to its hydrogen bonding and polarity. These findings highlight the significant impact of solvent characteristics on electrochemical processes.

KEYWORDS: Benzoquinone derivatives, DFT, Electron affinity, Reduction potential, Redox flow battery, Solvation-free energy, SMD solvation model

INTRODUCTION

Due to inequalities in power supply and demand, as well as a growing global population, the world's current energy production will quadruple by 2050 [1]. Fossil fuel use on a large scale has reduced the energy crisis while wreaking havoc on the environment [2, 3]. Large-scale energy storage devices are essential to replace fossil fuels and provide a reliable answer to these issues as the use of renewable energy sources such as wind, hydroelectric power, solar energy, and geothermal energy increases. Such renewable energy sources are environmentally benign and could be regarded as promising alternative energy sources for the world in the future [4]. In terms of dependability, safety, and cost, redox flow batteries (RFBs) offer a superior alternative to existing electrochemical energy storage technologies in medium- to large-scale stationary applications. In terms of cost, system flexibility, quick response, and safety concerns for large-scale applications, redox flow batteries show great advantages over other types of batteries, such as lead-acid and lithium-ion batteries, and are expected to have increasing commercial space through technological development in the future [5, 6].

*Corresponding authors. E-mail: mekonnen.ababayehu@aau.edu.et, yedilfana.setarge@aau.edu.et
This work is licensed under the Creative Commons Attribution 4.0 International License

Because of its modular design, superior scalability, and flexible operation, the redox flow battery is suitable for large-scale applications. This is because it can store much energy and power [7]. In redox flow batteries, as depicted in Figure 1 [8], the electroactive species are dissolved in an electrolyte, stored in a separate electrolyte tank, and then pumped to a power-converting electron reactor. The redox-active species make up the majority of a redox flow battery. The redox potential and solubility of electroactive species control the system's energy and power. The chemical stability, electrochemical reversibility, and reduction potential of redox materials all play a role in the overall effectiveness of redox flow batteries. Research has been conducted on several types of redox flow batteries, including organic and inorganic redox flow batteries [9]. Most redox flow batteries contain two electrolyte tanks, one of which stores electroactive materials for the positive electrode reaction (cathode) and the other of which stores electroactive materials for the negative electrode reaction (anode).

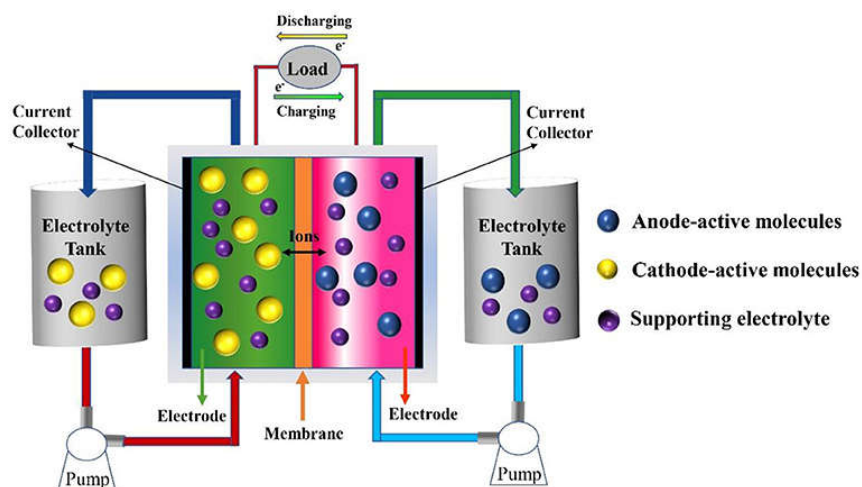


Figure 1. Schematic illustration of a redox flow battery [8].

Secondary batteries or rechargeable batteries are used as cathode active materials due to their high electrochemical reversibility and quick transfer of two electrons. For instance, the most promising redox-active organic compounds for stationary energy storage are quinone-based molecules, including an aqueous redox flow battery based on the redox chemistry of 9,10-anthraquinone-2,7-disulfonic with a Br/Br⁻ pair [10]. Quinone-based flow batteries can store more energy than conventional flow batteries because quinones transfer two-electron redox reactions in an aqueous solution. A previous study was conducted on the redox potential of quinone derivatives [11, 12]. Using the SMD solvation model, the electrochemical redox potentials of benzoquinone derivatives were investigated in both aqueous and non-aqueous solutions. The most promising organic redox potentials are quinones and their derivatives, which involve reversible redox reactions between lithium atoms and oxygen carbonyl groups [13, 14]. Depending on the substituent functional group, the redox properties and cycling performance of naphthylamide derivatives can work as a positive electrode for a lithium-ion battery, with a redox potential centered at 2.3 V to 2.9 V Li/Li⁺ [15]. Likewise, Assary and his colleagues used a computational method to study the redox potentials for the first and second reduction of anthraquinone derivatives [16].

In the early stage, Mitome *et al.* [17] investigated carbonyl-based redox-active organic compounds such as benzoquinone BQ, naphthoquinone NQ, and anthraquinone AQ. According to Huskinson *et al.* [18], those carbonyl redox-active compounds engage in two-electron, two-proton redox reactions in an aqueous solution and exhibit fast reversible redox reaction kinetics. Among carbonyl-based quinone molecules, the BQ molecule is the simplest and undergoes a reversible two-electron transfer reaction under neutral conditions. Redox reactions are a well-known form of electron transfer reaction that is relevant in a wide range of chemistry fields. Electrode potential simulations are particularly useful when experimental measurement is problematic due to complex chemical equilibrium. Because of their quick, simple, and cost-effective purposes, electrochemical techniques are now frequently used in many fields of chemistry for the study of electroactive substances [19, 20]. In electrochemistry, electronic structure methods and applications are powerful tools for obtaining certain physicochemical properties, as they have been implemented for various areas of study, including metal rechargeable batteries [20-22], spintronics [23, 24], and optoelectronics. When experimental observations are problematic, the inclination to calculate the redox potential properly using the theoretical method is favorable. The *ab initio* method has recently been utilized to determine the redox potential of various compounds in an aqueous solution [25].

In 2011, Senoh *et al.* [26] introduced a two-compartment cell design that utilized soluble benzoquinone derivatives as active materials for high-performance lithium secondary batteries. Their study demonstrated the stability and high capacity of various derivatives with different substituents over multiple charge-discharge cycles. Hooper-Burkhardt *et al.* [27] introduced a new Michael-reaction-resistant benzoquinone (BQ) derivative as a potential active material for aqueous organic redox flow batteries. They showed the high solubility and stable redox behavior of the BQ derivative, which is highly resistant to unwanted side reactions such as the Michael reaction. These studies highlight the importance of designing active materials with specific chemical functionalities to achieve desirable electrochemical properties. Luo *et al.* [28] emphasized the advantages of organic RFBs over other RFB technologies, such as high stability, low cost, and scalability, in their review. This suggests that organic redox flow batteries have promising potential as a technology for energy storage.

This study aimed to computationally determine the first- and second-reduction potentials of various BQ derivatives in three solvents with different dielectric constants. It explores important factors such as the solvation energy, salt effect, and functional group effect of BQ molecules, along with the contributions of EA and solvation energy to the redox potential of organic molecules during discharging. Additionally, the study calculates the HOMO and LUMO energies of BQ and its derivatives in both the gas and solvent phases.

Computational details

All calculations presented in this study were carried out using the density functional theory (DFT) tool implemented in the Gaussian 09 package. The B3LYP [29] functional level of theory with a split-valence 6-31G (d) basis set [30] was used to perform electronic property and geometry optimizations. The structures were optimized both in gas and in the solution phase (water, acetonitrile, and carbon tetrachloride) using the universal solvation model, SMD. This solvation model is a more realistic representation of the solvation effect compared to discrete solvent molecules and treated the solvent as a continuous dielectric [31].

Solvation free energy

The free energy of solvation in the reaction is obtained from the optimized gas-phase free energy and the free energy of solvation. The standard free energy of an electron is equal to zero at all temperatures [32]. The electron affinity in the gas phase can be calculated prior to the standard redox potential at 298 K and 1 atm [33] using equation 1.

For the general reaction:

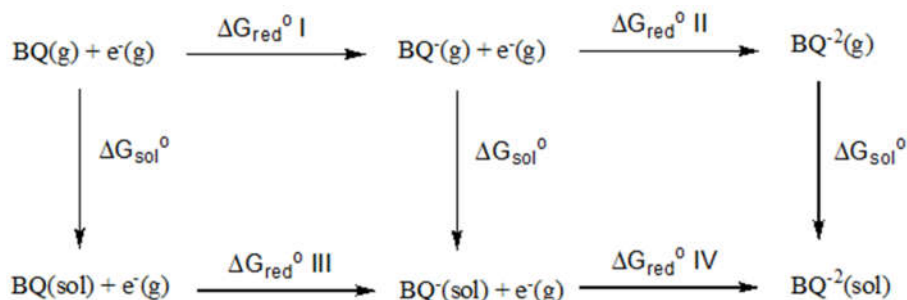


The electrode potential, E, can be used to express the quantity of free energy produced by electrochemical cells as well as the amount of energy required to do work.

$$\Delta G_{rxn}^0 = -nFE^0 \quad (2)$$

where ΔG_{rxn}^0 denotes the Gibbs free energy of solvation, n denotes the number of electrons transferred during charging/discharging, F denotes Faraday's constant, and E^0 denotes the cell's electrochemical redox potential.

The Born-Haber cycle changes all of the reactants from gas to a solution. The Gibbs free energy of solutions in a reaction is calculated using the Born-Haber cycle, as shown in Scheme 1:



Scheme 1. The thermodynamic quantity used to calculate solvation Gibbs free energy.

The redox potential (ΔE^{red}) of the active positive electrode material in solution with respect to a Li/Li⁺ reference electrode can be predicted from equation 3 [34].

$$\Delta E^{red} = -\frac{\Delta G_{sol}}{nF} - 1.24 V \quad (3)$$

$$i.e. \Delta G_{sol} = \Delta G_{sol}(BQ^-) - \Delta G_{sol}(BQ)_{neu} \quad (4)$$

where ΔG_{sol}^0 denotes the solvation-free energy. $\Delta G_{sol}(BQ^-)$ denotes the solvation energy of anionic species in a solution and, $\Delta G_{sol}(BQ)$ denotes the solvation-free energy of a neutral species, where n is the number of electrons transferred and F is the Faraday constant (96500 C/mol).

The constant 1.24 V indicates the redox potential of the Li/Li⁺ reference electrode [(-4.28 V [35, 36] Vs SHE (-3.04 V) Li/Li⁺]. All reduction potentials in this paper are reported with reference to Li/Li⁺ unless mentioned otherwise. The first and second reduction potentials of the benzoquinones were determined by considering the solvation effect using the SMD solvation model. The solvation-free energy corresponding to 1 atm and 298 K at the standard state was calculated while various electron-donating groups of benzoquinone derivatives were introduced, and their geometric structures were optimized to the ground state. The electronic properties, i.e., HOMO and LUMO energy levels, as well as the electron affinity of the active positive electrode materials, were also computed to rationalize the predicted reduction potentials.

HOMO-LUMO energies

The energies of the benzoquinone molecule and its electron-donating group in the ground states are determined for the highest occupied molecular orbital (HOMO) and lowest unoccupied molecular orbital (LUMO). Both HOMO and LUMO energies influence chemical stability. The energy difference between two molecules serves as a proxy for each molecule's chemical reactivity. According to Sajan and colleagues, frontier molecular orbital analysis was used to explain the optical and electrical properties of organic molecules [37, 38].

RESULTS AND DISCUSSION*Geometry optimizations*

The bond lengths with single and double bonds for carbon-carbon, carbon-oxygen, and carbon-hydrogen are represented as C – C, C – O, C – H, C = C, and C = O, respectively (Figure 2).

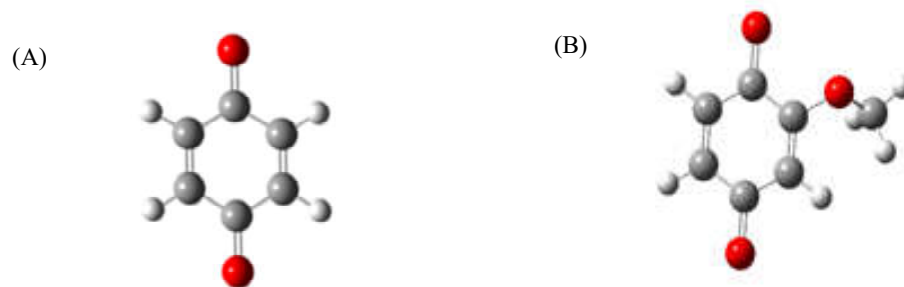


Figure 2. Labeling schemes for benzoquinone: (A) BQ and (B) BQ derivative (BQ-OCH₃). White, gray, and red colors represent hydrogen, carbon, and oxygen atoms, respectively.

Table 1. Calculated bond lengths and bond angles for 1,4-neutral (BQ) and anionic (BQ⁻) benzoquinone using a hybrid functional (B3LYP) compared to their available experimental findings. Values presented as previous findings are obtained from references[39, 40].

Bond parameters		BQ		BQ ⁻
		This work	Previous findings	This work
Bond length(Å)	C – C	1.3952	1.4810	1.3948
	C = C	1.3954	1.3440	1.3951
	C = O	1.4300	1.2250	1.4300
	C – H	1.0997	1.0890	1.0998
Bond angle(°)	C=C-C	120.0002	121.1000	119.8985
	C-C=O	119.9808	121.1000	119.9972
	C-C-C	120.0086	117.8000	119.9985
	C-C-H	119.9811	-	119.9840

The C-H, C=C, and C-C bond lengths indicated in Table 1 for the anionic benzoquinone molecules (BQ⁻) were calculated based on the geometric optimization of the neutral benzoquinone (BQ) molecule. The results revealed that the C=C and C-C bond lengths as well as the C-H bond length are shortened and lengthened very slightly, respectively.

The C = C has a bond energy (due to the presence of one sigma and one pi bond), while C-C and C-H have low bond energies (it contains one sigma bond). Higher bond energy typically correlates with shorter bond length because increased number of shared electron pairs pulls the bond atoms closer by reducing the reduction potential of benzoquinone. The redox properties of BQ correlates with its electronic properties like electro-affinity (EA), lowest unoccupied molecular orbitals (LUMO) and occupied molecular orbitals (HOMO) for the most stable state.

Solvent effects

One of the most important factors in determining a solute's solubility is its solvation-free energy [41]. Higher solvation-free energy suggests a more favorable interaction of the electron-donating group with the aqueous solvent (water) molecules, implying greater solubility. The optimized structures of BQ and its derivatives were used to estimate the first and second reduction potentials. Accordingly, Table 2 presents the calculated solvation-free energy (ΔG_{sol}) of benzoquinones in three distinct solvents (CCl₄, ACN, and H₂O) with various dielectric constants and polarities using the B3LY/6-31G(d) basis set combined with the SMD solvation model.

Table 2. Calculated free energies of solvation for benzoquinones.

	Benzoquinones	ΔG_{sol} (kcal/mol)		
		CCl ₄	ACN	H ₂ O
1	BQ	-61.69	-80.75	-89.72
2	2-Methylether BQ	-57.82	-76.90	-86.96
3	2-Methylamine BQ	-54.51	-72.88	-81.87
4	2-O-acyl BQ	-69.38	-84.63	-93.31
5	2-N-acyl BQ	-67.03	-82.61	-87.60
6	2-Amine BQ	-54.42	-73.51	-82.51

The solvent effect on the reduction potential depends on interactions between solute and solvent, such as solute-solvent hydrogen bonding, electron affinity, and solvation-free energy. Table 2 shows an increasing trend in solvation-free energy as follows CCl₄ < CAN < H₂O. The solvation-free energy of bare BQ in water, -89.72 kcal/mol, is higher than that of other bare BQ in three distinct solvents. This means that BQ is more soluble in water than in acetonitrile or carbon tetrachloride. The solvation-free energy of the ester-substituted BQ is higher than that of other electron-donating groups and bare BQ in the three solvents. As a result, adding an ester group to the functionalization of BQ can improve the interaction between the solute and solvents. Because the solvent phase influences the reduction potential through the solvation effect and electron affinity [42], the effect of the solvent phase's dielectric constant on the redox potential was also addressed. The average solvation-free energy of water (-86.90 kcal/mol) is higher than that of the other two solvents. The dielectric constant also has a comparable influence on the redox potential for the BQ functional group. The redox potential rises from a low dielectric constant to a high dielectric constant, and it stays constant beyond a certain point.

Prediction of reduction potentials

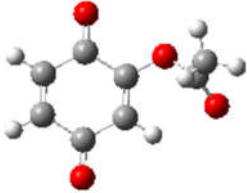
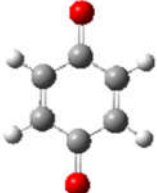
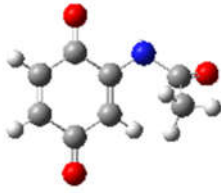
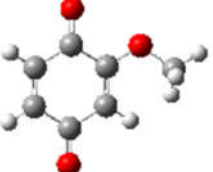
There are two basic characteristics of the redox properties of organic compounds containing carbonyls, such as quinone employed as cathode active material in redox flow batteries [43, 44]. The first is that organic molecules would continue to exhibit cathodic activity while having positive redox potentials up until each carbonyl could bond with one Li, and cathodic activity would mostly depend on solvation energy. Investigated compounds with negative solvation energies (solvation-free energy at neutral state > solvation-free energy at anion state) would have positive redox potentials and be cathodically active.



The redox potential of a molecule is a measurement of its ability to gain or lose electrons. The thermodynamic cycle that connects the gas phase and solvent processes should be used to compute the redox potentials [45].

As shown in Table 3, the first-reduction potential (E^1_{red}) and second-reduction potential (E^2_{red}) of benzoquinones in the three solvents increase from carbon tetrachloride through acetonitrile to water. This is because of hydrogen bonding, HOMO energies, polarity, and the solvent's dielectric constant.

The correlation of the electron-donating group vs. the reduction potential of benzoquinones is shown in Figure 3. The reduction potentials of benzoquinones were calculated with respect to Li^+/Li .

Table 3. Calculated first (E^1_{red}) and second (E^2_{red}) reduction potentials (V) of benzoquinones using the B3LYP/6-31G (d) level of theory in three solvents.

Benzoquinones	H ₂ O		ACN		CCl ₄	
	E^1_{red}	E^2_{red}	E^1_{red}	E^2_{red}	E^1_{red}	E^2_{red}
	2.81	2.27	2.43	1.63	1.77	0.56
	2.65	2.01	2.26	1.43	1.44	0.33
	2.56	2.04	2.35	1.49	1.67	0.01
	2.53	1.92	2.09	1.32	1.27	0.43

	2.34	1.78	1.95	1.22	1.22	0.53
	2.29	1.77	1.92	1.21	1.22	0.01

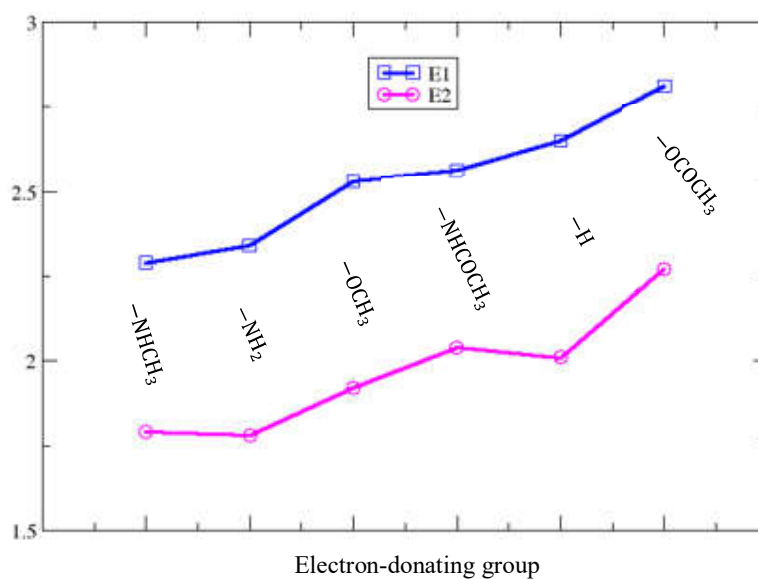


Figure 3. The predicted E_{red}^1 and E_{red}^2 of BQ and its substituent at the B3LYP functional by using a 6-31/G (d) basis set.

The results revealed that the reduction potentials, E_{red}^1 and E_{red}^2 , of the benzoquinones decrease upon substitution of the different electron-donating groups at the ortho position except for the ester substituent. The corresponding lithiation redox potentials of quinones are greatly influenced by their functional groups. Li-O bonds are formed more easily when the initial Li-ion (Li^+) is bound due to the increased redox activity of the electron-donating group at the ortho position of the carbonyl group. The higher reduction potentials indicated that the carbonyl group of esters at the ortho position has a greater potential for electrostatic attraction to the positively charged lithium ion.

The effects of salt on the reduction potentials

Due to their high redox potential and theoretical capacity [46], benzoquinone compounds have shown tremendous promise as cathode-active materials in lithium-ion batteries [47]. BQ is the cathode active material in a rechargeable lithium-ion battery and will undergo a stepwise redox process involving two electrons. In the discharge process, this can be seen as the production of two reduction potentials or plateaus. Here, lithium atoms were assumed to interact with the redox-active sites step by step. The effect of salts (BF_3 and PF_5) on the first- and second-reduction potentials of BQ is indicated in Table 4.

Table 4. The effects of salts on the first and second reduction potential of benzoquinone.

Salt effect	E^1_{red}	E^2_{red}	Complexation-free energy (eV)
No salt	2.65	2.01	NA
BF_3	3.91	3.72	-0.1779
PF_5	3.81	3.76	-4.9500
2BF_3	3.99	3.84	0.1500
2PF_5	3.66	3.56	-0.1200

The results obtained for benzoquinone are in excellent agreement with the previous theoretical reduction (no salt) [34]. The calculated free energy of the complex formation of the salt effect (Lewis acid) with benzoquinone is also shown in Table 4. The first and second reduction potentials were considered with respect to Li/Li^+ as a reference electrode. For the salt mentioned above, the predicted free energies of complex formation were also computed. Benzoquinone forms complexes with salts. The free energies of BQ-salt complex formation were calculated from the free energies of the complex and the sum of the free energies of BF_3 and BQ in solution.

The coordination of salt and salt decomposition products raises the estimated first- and second-reduction potentials by 0.80 to 1.60 V. The electron affinity of BQ increases when it forms complexes with electron-withdrawing group salts such as BF_3 and PCl_5 , which explains why the reduction potential increased significantly. These compounds bind to BQ with a mild exergonic effect. The last entry was obtained from an earlier published theoretical measurement [34]. The calculated first (2.65 V), and second (2.01 V), the reduction potentials of BQ are in excellent agreement with the earlier theoretical reduction potential values.

Effects of a functional group on the reduction potential of BQ

The electronic properties of extra functional groups influence the redox properties of the investigated molecule [48]. To predict the redox properties of active compounds, it is necessary to understand how the electronic transfer mechanism of functional groups affects the BQ redox window. The electronic structure properties of a redox-active molecule determine its redox behavior.

The computed first (E^1_{red}) and second (E^2_{red}) reduction potentials of six benzoquinones without salt molecules were studied, as shown in Table 3. For instance, the first and second reduction potentials of bare benzoquinone are 2.65 V vs. Li/Li^+ (standard reduction potential without Li/Li^+ , 3.89 V) and 2.01 V vs. Li/Li^+ (standard reduction potential without Li/Li^+ , 3.25 V), respectively.

HOMO-LUMO energies

The HOMO-LUMO energies have an impact on a molecule's ability to react chemically. During a chemical reaction, the HOMO is the ability to donate an electron, and its energy is proportional to the ionization potential. The energy gap between LUMO and HOMO could determine the

charge transfer interaction within a benzoquinone molecule [49]. The delocalization of pi electrons, which results in a reduced HOMO-LUMO gap, makes it simple for an electron to transition from a lower energy level to a higher energy level with a similar energy level. The lower the HOMO-LUMO gap value, the higher the reactivity of the studied compounds. The chemical X = -OCOCH₃ is more stable (less reactive) and more reactive in X = -NHCH₃.

The chemical activity of the BQ molecule is reflected in the HOMO-LUMO gap. The charge transfer interaction inside the investigated molecule is shown by a decrease in the HOMO-LUMO gap. The stability of the species investigated decreases in the following order. -OCOCH₃ > -H > -OCH₃ > -NHCOCH₃ > -NH₂ > -NHCH₃ solvent in water, which is the same in the gas phase.

Table 5. The HOMO-LUMO energy gap, which is computed at the B3LYP/6-31G (d) level.

	Substituents	Parameter				
		HOMO (eV)	LUMO (eV)	E _{gap} (eV)	IP (eV)	EA (eV)
GAS	-OCOCH ₃	-7.60	-3.80	3.81	7.60	3.80
	-H	-7.36	-3.54	3.82	7.36	3.52
	-OCH ₃	-7.12	-3.22	3.90	7.12	3.22
	-NHCOCH ₃	-6.17	-3.15	3.02	6.17	3.15
	-NH ₂	-6.32	-3.11	3.21	6.32	3.11
	-NHCH ₃	-6.00	-3.00	3.00	6.00	3.00
CCl4	-OCOCH ₃	-7.48	-3.63	3.85	7.48	3.63
	-H	-7.22	-3.38	3.84	7.22	3.38
	-OCH ₃	-6.94	-3.11	3.83	6.94	3.11
	-NHCOCH ₃	-6.45	-3.11	3.34	6.45	3.11
	-NH ₂	-6.13	-2.97	3.16	6.13	2.97
	-NHCH ₃	-5.83	-2.89	2.94	5.83	2.89
Acetonitrile	-OCOCH ₃	-7.32	-3.40	3.92	7.32	3.40
	-H	-7.09	-3.22	3.87	7.09	3.22
	-OCH ₃	-6.77	-3.02	3.75	6.77	3.02
	-NHCOCH ₃	-6.68	-3.23	3.45	6.68	3.23
	-NH ₂	-5.95	-2.88	3.09	5.97	2.88
	-NHCH ₃	-5.69	-2.81	2.87	5.69	2.82
Water	-OCOCH ₃	-7.59	-3.59	4.00	7.59	3.59
	-H	-7.37	-3.43	3.90	7.37	3.43
	-OCH ₃	-6.93	-3.28	3.65	6.93	3.28
	-NHCOCH ₃	-6.91	-3.46	3.45	6.91	3.46
	-NH ₂	-6.10	-3.10	3.00	6.10	3.10
	-NHCH ₃	-5.85	-3.05	2.80	5.85	3.05

Chemical reactivity, on the other hand, decreases in the reverse order, -OCOCH₃ < -H < -OCH₃ < -NHCOCH₃ < -NH₂. The corresponding energy levels of the frontier molecular orbital for the benzoquinones are shown in Figure 4. Based on the frontier molecular orbital investigation, electron transfer would occur between the HOMO and LUMO.

As shown in Table 5, the calculated LUMO and HOMO molecular orbitals (MOs) of the BQ derivatives are primarily dispersed on the BQ core and the substituents, respectively. While the substituents can act as a donor, the BQ core can behave as an acceptor. A split electron density distribution between HOMO and LUMO may result from the donor-acceptor configuration of this compound. The electron transport capability of the investigated molecule is caused by this separation. The redox properties of the six quinone derivatives can be explained by correlating them with their electronic structures, specifically LUMO and HOMO, in both stable Li binding cases. As shown in Figure 5, the redox potential has a direct relationship with the LUMO, HOMO, and HOMO-LUMO gap. The greater positive value of the HOMO-LUMO gap would be associated with higher redox potential, whereas the more negative values for LUMO and HOMO

would have higher redox potentials for Quinones with more reductive capacity. Similar observations have been consistently reported in other studies, as presented in Table 5 [43]. Therefore, $-\text{NHCH}_3$ (low band gap) and $-\text{OCOCH}_3$ (high band gap) can be related to the high and low chemical reactivity, respectively.

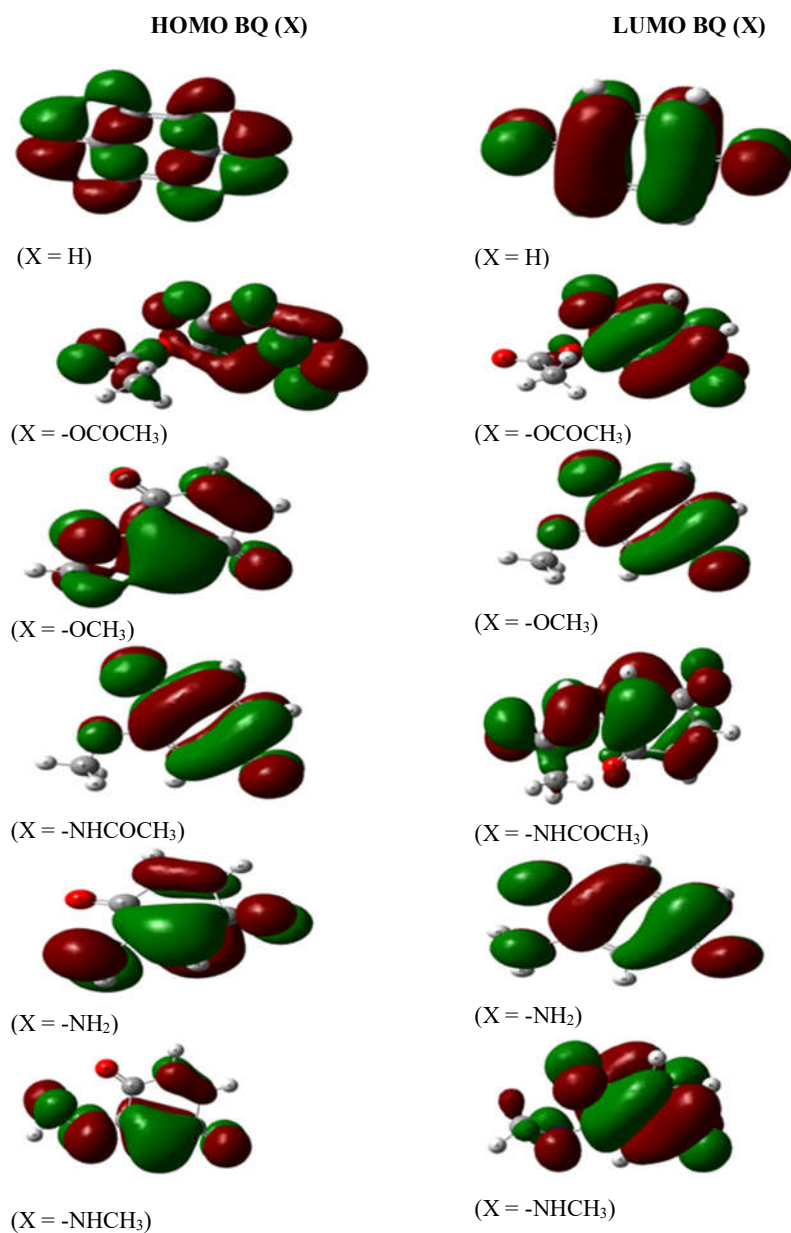


Figure 4. Shapes of frontier molecular orbitals of BQ and its derivatives.

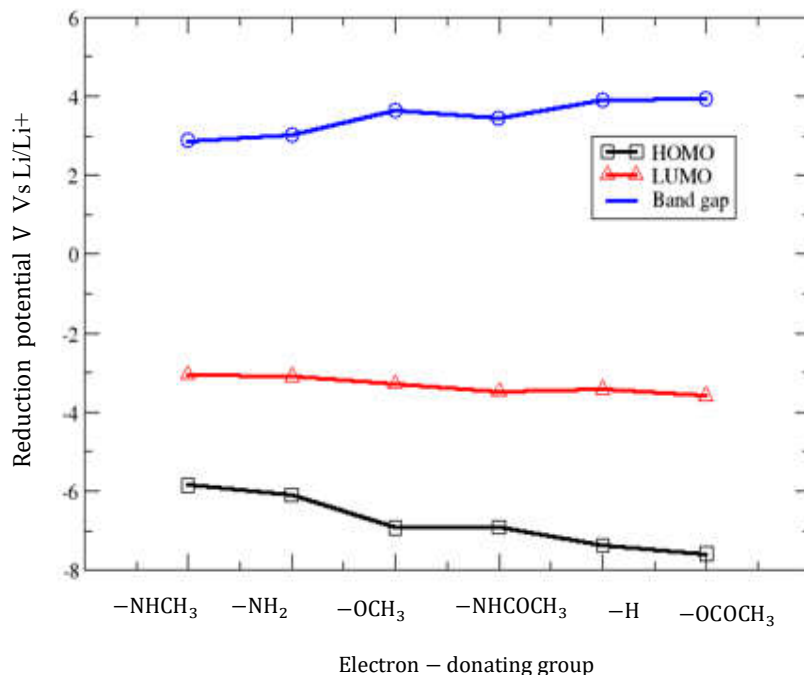


Figure 5. The computed HOMO-LUMO energies of BQ derivatives at the B3LYP/DFT level of theory using a 6-31G/d basis set.

CONCLUSION

DFT calculations at the B3LYP/6-31G(d) level of theory are employed to determine the first and second reduction potentials of benzoquinone and its derivatives, both in the gas phase and in three different solvents. The solvation energies of these organic molecules are obtained using the SMD solvation model. BQ derivatives are generated by applying electron-donating substituents (-NHCH₃, -NH₂, -OCH₃, -NHCOCH₃, and -OCOCH₃) to the parent benzoquinone molecule. In this paper, the effects of selected electron-donating substituents, HOMO-LUMO energies, solvation-free energy, and lithium salts on the first- and second-reduction potentials of benzoquinones are investigated. The results demonstrated that the molecule BQ-NHCH₃ has a low HOMO-LUMO energy gap in both the gas and solvent phases, making it kinetically less stable but exhibiting a high level of chemical reactivity in all the solvents under investigation and the gas phase. Moreover, -OCOCH₃-substituted BQ exhibited the highest first- and second-reduction potentials with values of 2.81 V (2.27 V) mainly due to an increase in BQ's electron affinity, these values further improved to 3.99 V (3.84 V) upon the addition of 2BF₃ salt. The reduction potentials were significantly influenced by salt and salt decomposition products or Lewis acid substituents. The study shows that BF₃ salt significantly improved the reduction potentials of BQ derivatives due to an increase in the electron affinity of BQ when it forms complexes with electron-withdrawing salts. As a result of its hydrogen bonding, polarity, and dielectric constant, water has been proven to be the preferable solvent for boosting the reduction potential, followed by acetonitrile and carbon tetrachloride.

Conflict of interest

The authors declare no conflict of interest.

Availability of data

The data that support the findings of this study are presented in this article.

ACKNOWLEDGMENTS

This work was supported by a thematic research project (grant no. TR/036/2021) funded by Addis Ababa University. Computer resources for the study were kindly provided by the Center for Functional Nanomaterials (CFN), which is a U.S. Department of Energy Office of Science User Facility, at Brookhaven National Laboratory under Contract No. DE-SC0012704 and project number 308379 and 312563, and the Ethiopian Education and Research Network (EthERNet) at the Ethiopian Ministry of Education. G.A. N would like to acknowledge financial support from the Ethiopian Ministry of Education. Y.S.M. acknowledges support from the ICTP through the Associates Programme (2020-2025).

REFERENCES

1. Pan, F.; Wang, Q. Redox species of redox flow batteries: A review. *Mol.* **2015**, *20*, 20499–20517.
2. Holdren, J.P. Global environmental issues related to energy supply: The environmental case for increased efficiency of energy use. *Energy* **1987**, *12*, 975–992.
3. Gemechu, D.N.; Mohammed, A.M.; Redi, M.; Bessarabov, D.; Mekonnen, Y.S.; Obodo, K.O. First principles-based approaches for catalytic activity on the dehydrogenation of liquid organic hydrogen carriers: A review. *Int. J. Hydrog. Energy* **2023**, *48*, 33186–33206.
4. Maddukuri, S.; Malka, D.; Chae, M.S.; Elias, Y.; Luski, S.; Aurbach, D. On the challenge of large energy storage by electrochemical devices. *Electrochim. Acta* **2020**, *354*, 136771.
5. Olabi, A.G.; Allam, M.A.; Abdelkareem, M.A.; Deepa, T.D.; Alami, A.H.; Abbas, Q.; Alkhalidi, A.; Sayed, E.T. Redox flow batteries: Recent development in main components, emerging technologies, diagnostic techniques, large-scale applications, and challenges and barriers. *Batteries* **2023**, *9*, 409.
6. Zhang, H.; Sun, C. Cost-effective iron-based aqueous redox flow batteries for large-scale energy storage applications: A review. *J. Power Sources* **2021**, *493*, 229445.
7. Wang, W.; Luo, Q.; Li, B.; Wei, X.; Li, L.; Yang, Z. Recent progress in redox flow battery research and development. *Adv. Funct. Mater.* **2013**, *23*, 970–986.
8. Zhong, F.; Yang, M.; Ding, M.; Jia, C.; Ding, M. Organic electroactive molecule-based electrolytes for redox flow batteries: Status and challenges of molecular design. *Front. Chem.* **2020**, *8*, 1–14.
9. Hu, B.; Luo, J.; DeBruler, C.; Hu, M.; Wu, W.; Liu, T.L. *Redox-Active Inorganic Materials for Redox Flow Batteries in Encyclopedia of Inorganic and Bioinorganic Chemistry*, 2nd ed.; Scott, R.A. (Ed.), Wiley: New York; **2019**; pp. 1–25.
10. Er, A.; Süleyman; Suh, C.; Marshak, M.P.; Aspuru-Guzik, A. Computational design of molecules for an all-quinone redox flow battery. *Chem. Sci.* **2015**, *6*, 885–893.
11. Namazian, M.; Coote, M.L. Accurate calculation of absolute one-electron redox potentials of some para-quinone derivatives in acetonitrile. *Phys. Chem. Chem. Phys.* **2007**, *3*, 7227–7232.
12. Namazian, M.; Siahrostami, S.; Coote, M.L. Electron affinity and redox potential of tetrafluoro-*p*-benzoquinone: A theoretical study. *J. Fluorine Chem.* **2008**, *129*, 222–225.
13. Gerhardt, M.R.; Galvin, C.J.; Huskinson, B.; Marshak, M.P.; Suh, C.; Chen, X. A metal-free organic–inorganic aqueous flow battery. *Nature* **2014**, *505*, 195–198.

14. Kim, K.C.; Liu, T.; Lee, S.W.; Jang, S.S. First-principles density functional theory modeling of Li binding: Thermodynamics and redox properties of quinone derivatives for lithium-ion batteries. *J. Am. Chem. Soc.* **2016**, *138*, 2374–2382.
15. Kim, K.C.; Liu, T.; Jung, K.H.; Lee, S.W.; Soon, S. Unveiled correlations between electron affinity and solvation in redox potential of quinone-based sodium-ion batteries. *Energy Storage Mater.* **2019**, *19*, 242–250.
16. Guin, P.S.; Das, S.; Mandal, P.C. Electrochemical reduction of quinones in different media: A review. *Open Access J. Chem.* **2011**, 2011, 86–89.
17. Wedege, K.; Dražević, E.; Konya, D.; Benti, A. Organic redox species in aqueous flow batteries: Redox potentials, chemical stability, and solubility. *Sci. Rep.* **2016**, 39101, 1–13.
18. Gong, K.; Fang, Q.; Gu, S.; Fong, S.; Li, Y.; Yan, Y. Nonaqueous redox-flow batteries: Organic solvents, supporting electrolytes, and redox pairs. *Energy Environ. Sci.* **2015**, *8*, 3515–3530.
19. Mindia Ali, A.; Waziri, I.; Garba, H. *Recent Developments in the Electron Transfer Reactions and Their Kinetic Studies in Chemical Kinetics and Catalysis - Perspectives, Developments and Applications*; Khattak, R. (Ed.), IntechOpen: Online Publication; **2024**.
20. Lee, J.; Srimuk, P.; Fleischmann, S.; Su, X.; Hatton, T.A.; Presser, V. Redox-electrolytes for non-flow electrochemical energy storage: A critical review and best practice. *Prog. Mater. Sci.* **2019**, *101*, 46–89.
21. Gurmesa, G.S.; Benti, N.E.; Chaka, M.D.; Tiruye, G.A.; Zhang, Q.; Mekonnen, Y.S.; Geffe, C.A. Fast 3D-lithium-ion diffusion and high electronic conductivity of $\text{Li}_2\text{MnSiO}_4$ surfaces for rechargeable lithium-ion batteries. *RSC Adv.* **2021**, *11*, 9721–9730.
22. Gurmesa, G.S.; Teshome, T.; Benti, N.E.; Tiruye, G.A.; Datta, A.; Mekonnen, Y.S.; Chernet Amente Geffe, C.A. Rational design of biaxial tensile strain for boosting electronic and ionic conductivities of $\text{Na}_2\text{MnSiO}_4$ for rechargeable sodium-ion batteries. *ChemistryOpen* **2022**, *11*, e202100289.
23. Begna, W.B.; Gurmesa, G.S.; Zhang, Q.; Geffe, C.A. A DFT+U study of site-dependent Fe-doped TiO_2 diluted magnetic semiconductor material: Room-temperature ferromagnetism and improved semiconducting properties. *AIP Adv.* **2022**, *12*, 025002.
24. Begna, W.B.; Gurmesa, G.S.; Geffe, C.A. Ortho-atomic projector assisted DFT+U study of room temperature ferro- and antiferromagnetic Mn-doped TiO_2 diluted magnetic semiconductor. *Mater. Res. Express* **2022**, *9*, 076102.
25. Fu, Y.; Liu, L.; Yu, H.-Z.; Wang, Y.-M.; Guo, Q.-X. Quantum-chemical predictions of absolute standard redox potentials of diverse organic molecules and free radicals in acetonitrile. *J. Am. Chem. Soc.* **2005**, *127*, 7227–7234.
26. Senoh, H.; Yao, M.; Sakaebe, H.; Yasuda, K.; Siroma, Z. A two-compartment cell for using soluble benzoquinone derivatives as active materials in lithium secondary batteries. *Electrochim. Acta* **2011**, *56*, 10145–10150.
27. Hooper-Burkhardt, L.; Krishnamoorthy, S.; Yang, B.; Murali, A.; Nirmalchandar, A.; Surya Prakash, G.K.; Narayanan, S.R. A new Michael-reaction-resistant benzoquinone for aqueous organic redox flow batteries. *J. Electrochem. Soc.* **2017**, *164*, A600–A607.
28. Luo, J.; Hu, B.; Hu, M.; Zhao, Y.; Liu, T.L. Status and prospects of organic redox flow batteries toward sustainable energy storage. *ACS Energy Lett.* **2019**, *4*, 2220–2240.
29. Pérez-Jiménez, Á.J.; Pérez-Jordá, J.M.; Pastor-Abia, L.; Sancho-García, J.C. New correlation energy functionals with explicit dependence on the number of electrons. *J. Chem. Phys.* **2002**, *116*, 10571–10576.
30. Mohammad-Shiri, H.; Ghaemi, M.; Riahi, S.; Akbari-Sehat, A. Computational and electrochemical studies on the redox reaction of dopamine in aqueous solution. *Int. Res. J. Pure Appl. Chem.* **2011**, *6*, 317–336.

31. Marenich, A.V.; Cramer, C.J.; Truhlar, D.G. Universal solvation model based on solute electron density and on a continuum model of the solvent defined by the bulk dielectric constant and atomic surface tensions. *J. Phys. Chem. B* **2009**, *113*, 6378–6396.
32. Winget, P.; Cramer, C.J.; Truhlar, D.G. Computation of equilibrium oxidation and reduction potentials for reversible and dissociative electron-transfer reactions in solution. *Theor. Chem. Acc.* **2004**, *112*, 217–227.
33. Liptak, M.D.; Gross, K.C.; Seybold, P.G.; Feldgus, S.; Shields, G.C. Absolute pK_a determinations for substituted phenols. *J. Am. Chem. Soc.* **2002**, *124*, 7314–7319.
34. Bachman, J.E.; Curtiss, L.A.; Assary, R.S. Investigation of the redox chemistry of anthraquinone derivatives using density functional theory. *J. Phys. Chem. C* **2014**, *118*, 8852–8860.
35. Isse, A.A.; Gennaro, A. Absolute potential of the standard hydrogen electrode and the problem of interconversion of potentials in different solvents. *Chem. Phys. Lett.* **2010**, *114*, 7894–7899.
36. Kelly, C.P.; Cramer, C.J.; Truhlar, D.G. Aqueous solvation free energies of ions and ion-water clusters based on an accurate value for the absolute aqueous solvation free energy of the proton. *J. Phys. Chem. B* **2006**, *110*, 16066–16081.
37. Padmaja, L.; Ravikumar, C.; Sajan, D.; Hubert Joe, I.; Jayakumar, V.S.; Pettit, G.R.; Nielsen, O.F. Density functional study on the structural conformations and intramolecular charge transfer from the vibrational spectra of the anticancer drug combretastatin-A2. *J. Raman Spectrosc.* **2009**, *40*, 419–428.
38. Nigatu, D.; Mohammed, A. Computational investigation on dipyrido[3,2-a:2',3'-c]phenazine and its cobalt(II) complex. *Int. Res. J. Pure Appl. Chem.* **2017**, *14*, 1–8.
39. Hagen, K.; Hedberg, K. Reinvestigation of the molecular structure of gaseous *p*-benzoquinone by electron diffraction. *J. Chem. Phys.* **1973**, *59*, 158–162.
40. Mohandas, P.; Umopathy, S. Density-functional studies on the structure and vibrational spectra of transient intermediates of *p*-benzoquinone. *J. Phys. Chem. A* **1997**, *101*, 4449–4459.
41. Palmer, D.S.; Llinàs, A.; Morao, I.; Day, G.M.; Goodman, J.M.; Glen, R.C.; Mitchell, J.B.O. Predicting intrinsic aqueous solubility by a thermodynamic cycle. *Mol. Pharm.* **2008**, *5*, 266–279.
42. Brus, L.E. A simple model for the ionization potential, electron affinity, and aqueous redox potentials of small semiconductor crystallites. *J. Chem. Phys.* **1983**, *79*, 5566–5571.
43. Park, J.H.; Liu, T.; Kim, K.C.; Lee, S.W.; Jang, S.S. Systematic molecular design of ketone derivatives of aromatic molecules for lithium-ion batteries: First-principles DFT modeling. *ChemSusChem* **2017**, *10*, 1584–1591.
44. Kim, K.C.; Liu, T.; Lee, S.W.; Jang, S.S. First-principles density functional theory modeling of Li binding: Thermodynamics and redox properties of quinone derivatives for lithium-ion batteries. *J. Am. Chem. Soc.* **2016**, *138*, 2374–2382.
45. Babu, N.S.; Tedesse, S.; Lelisho, T.A. Computational and electrochemical studies on the redox reaction of quinoxalin-2(H)-one and its derivatives in aqueous solution. *Res. Artic.* **2013**, *5*, 61–69.
46. Zhao, J.C.Q.; Miao, L.; Ma, M.; Liu, L. Theoretical study on the lithiation mechanism of benzoquinone-based macrocyclic compounds as cathodes for lithium-ion batteries. *Phys. Chem. Chem. Phys.* **2019**, *21*, 11004–11010.
47. Miao, L.; Liu, L.; Shang, Z.; Li, Y.; Lu, Y.; Cheng, F.; Chen, J. Structure-electrochemical property relationship of quinone electrodes for lithium-ion batteries. *Phys. Chem. Chem. Phys.* **2018**, *20*, 13478–13484.
48. Aspuru-Guzik, A. Computational design of molecules for an all-quinone redox flow battery. *Chem. Sci.* **2015**, *6*, 845–1592.

49. Miar, M.; Shiroudi, A.; Pourshamsian, K.; Olliaey, A.R.; Hatamjafari, F. Theoretical investigations on the HOMO-LUMO gap and global reactivity descriptors, natural bond orbital, and nucleus-independent chemical shifts analyses of 3-phenylbenzo[d]thiazole-2(3H)-imine and its para-substituted derivatives. *J. Chem. Res.* **2021**, 1–12.